Title	Ceramic Coating of Titanium by Pulsed YAG Laser(Physics, Process & Instrument)
Author(s)	Wehr, Muryel; Katayama, Seiji; Matsunawa, Akira
Citation	Transactions of JWRI. 1987, 16(1), p. 43-49
Version Type	VoR
URL	https://doi.org/10.18910/11242
rights	
Note	

Ceramic Coating of Titanium by Pulsed YAG Laser†

Muryel WEHR*, Seiji KATAYAMA** and Akira MATSUNAWA***

Abstract

With the object of improving erosion and wear resistance of titanium (Ti), a feasibility of the formation of hard ceramics such as carbides, borides and nitrides on its surface was investigated by irradiating powder-predeposited Ti sheet with a pulsed YAG laser under argon (Ar) or nitrogen (N_2) atmosphere. As a result, a flat surface of laser-melted zone was formed depending on a proper amount of powders under appropriate laser irradiation conditions, and the fusion zone generally exhibited a dendritic microstructure (with some inclusions in the case of boron or boride powders). The analyses of X-ray diffractometer results confirmed that carbides, borides and nitrides were formed in addition to alpha-Ti phase in the vicinity of the surface, and probably constituted the dendrites in the fusion zone. Vickers surface hardnesses of fusion zones measured under 100 g load were increased and varied in the range of about 500 to 1200 kg/mm² in Ar atmosphere and about 1000 to 1700 kg/mm² in N_2 environment, although Ti sheet had a hardness of about 200 to 250 kg/mm². Hence, the utilization of N_2 atmosphere instead of Ar during laser irradiation increased the surface hardness of about 500 kg/mm² for powder compositions such as C, TiC, WC, SiC, B and TiB_2. Some inclusions in boride coatings indicated hardness values of more than 2000 kg/mm².

KEY WORDS: (Laser) (Ceramic Coating) (Titanium) (Powder Deposition) (Gas Atmosphere) (Hardness) (Dendritic Microstructure) (Carbides) (Borides) (Melted Zones)

1. Introduction

Titanium (Ti) and its alloys are being considered as particularly effective in aerospace applications[1] and other high performance structures as a result of their high strength to weight ratio and good corrosion resistance[2]. In order to improve the erosion and wear resistance of Ti, ceramics[3),4)] were generally chosen as a coating, due to their high hardness and stability at higher operating temperatures. The high hardness of carbides[6),7)], nitrides[8] and borides[9] is well suited to erosion and wear resistance.

Ceramics coating of titanium is performed by laser surface alloying. This material processing method utilizes the high power density available from focused laser sources to melt coatings and a portion of the underlying substrate[5]. Laser surface alloying may be realized by several methods such as powder deposition. Powder deposition methods may be broadly classified as predeposition (put down on the substrate in a separate step before the laser treatment[5]) and codeposition (injected into the melt at the time of laser treatment[6] or into the laser beam over the working piece[10]).

This paper describes the process of these ceramic coatings on pure Ti by pulsed YAG laser, using a predeposition method, and results concerning morphology, coatings composition and hardness.

2. Experimental Procedure

2.1 Process

The base material was commercially pure Ti sheet ($3^t \times 15^w \times 15^l$mm). Powder compositions used were C, TiC, SiC, WC, B, TiB_2, WB and mixed B + C, and their size characteristics are given in **Table 1**.

After polishing the Ti substrate with 400 Emery paper and cleaning with acetone, powders were put down with an acrylic liquid. Samples were then irradiated by a pulsed YAG laser, under Ar or N_2 atmosphere, as shown in **Fig. 1**.

The pulsed YAG laser (Control Laser, Model 428; maximum average power: 200 W) beam was focused with a 120 mm focal length lens and oriented perpendicularly to the sample surface. The main laser irradiation conditions used are also indicated in Fig. 1.

2.2 Samples characterization

Microstructure of coating layer was observed by optical microscope and scanning electron microscope (SEM). Phases formed were analyzed by energy dispersive X-ray spectrometer (EDX) and determined by X-ray diffractometry (Cu-K_α), and hardness was measured with a Vickers diamond under 100 g load (Hv).

† Received on May 6, 1987

* Visiting Researcher
** Research Instructor
*** Professor

Transactions of JWRI is published by Welding Research Institute of Osaka University, Ibaraki, Osaka 567, Japan

Table 1 Powders sizes (μm)

Powder	C	TiC	SiC	WC	C + B	B	TiB_2	WB
Size	0.5	0.5	15;85	0.8	<10	10	1.5	2

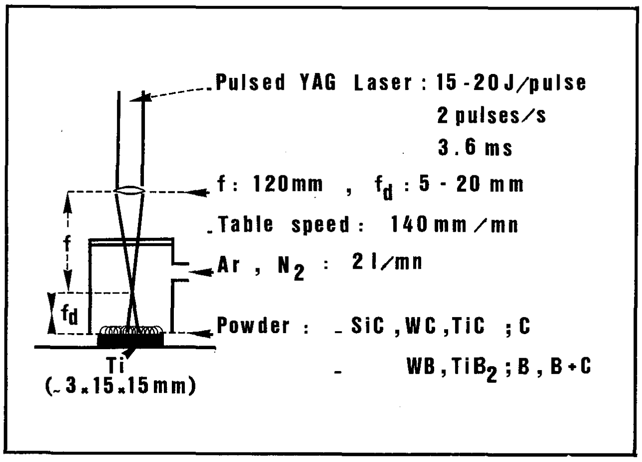

Fig. 1 Experimental conditions.

3. Results and Discussion

3.1 Geometry of laser fusion zone

In the case of this powder-predeposited method, it was difficult to melt only ceramic powders, and therefore ceramic coatings were produced by fusing both powders and Ti substrate together. The geometry of laser-irradiated part depended largely upon operating conditions such as laser power density (energy and defocused distance) and powder size, deposition thickness and composition. When the power density was not sufficient, powder melting did not occur, but on the contrary, if it was too high, a hole appeared in the substrate. Namely, it was necessary to find out optimum laser irradiation conditions for the formation of a fusion zone having a flat surface.

Figure 2 shows the surface appearance of fusion zone produced by pulsed YAG laser shots in Ar atmosphere, in the case of titanium sheet with TiC powder predeposited. Flat surfaces of fusion spots with an overlapping ratio of about 40% are seen.

Figure 3 shows cross section of SiC powder-predeposited Ti sheet after laser treatment. The melted zone was about 150μm in depth. Fusion zone depths were less than 350μm for any powder under the laser irradiation conditions for flat surface formation.

3.2 Microstructure of laser fusion zone

Figure 4 (a) to (f) exhibit cross-sectional microstructures of laser-melted Ti sheets with TiC, WC and B powders predeposited in Ar and N_2 atmosphere. Laser-melted zones, i.e. coatings, show mainly a dendritic microstructure. Fig. 4 (a), (b) and (c) present typical dendrites morphologies named "skeleton", "flake" and "rod" shape. The microstructures observed in Ar atmosphere are summarized for different powders in **Table 2.** It appears that dendrites characteristics depend on powder compositions: "skeleton" and "flake" shapes in the case of carbides and mainly "rod" form in the case of borides. Dendrites length reached values as high as 40 and 70μm

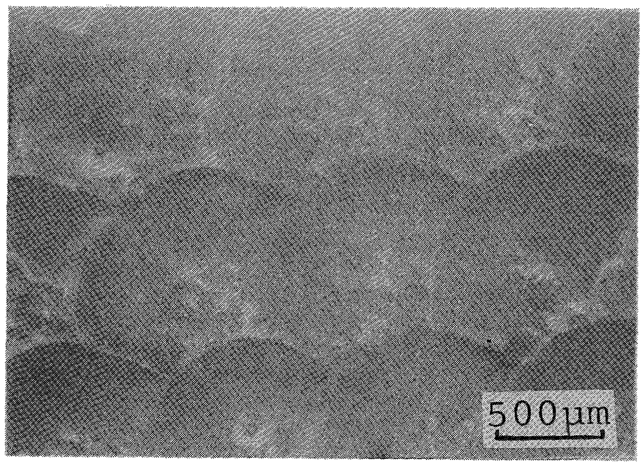

Fusion zone surface TiC powder/Ti/Ar

Fig. 2 Surface appearance of fusion zone produced by pulsed YAG laser shots, in argon atmosphere, on TiC powder (<1μm size) predeposited titanium.

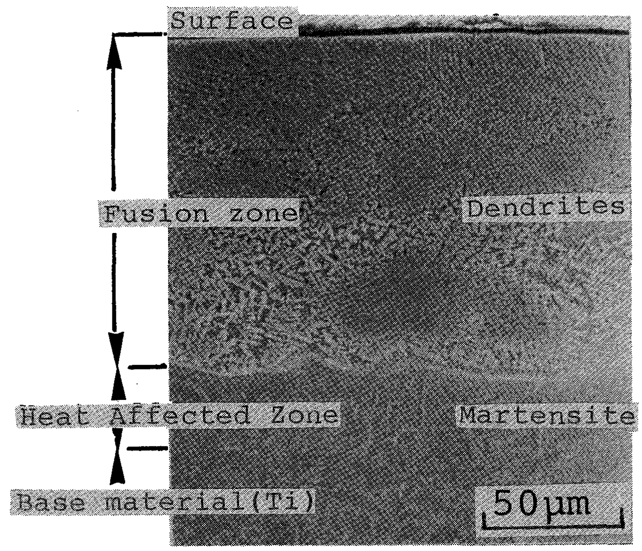

Fusion zone cross section SiC powder/Ti/Ar

Fig. 3 Fusion zone cross-section of SiC-predeposited Ti, irradiated by YAG laser in Ar atmosphere (SiC/Ti/Ar).

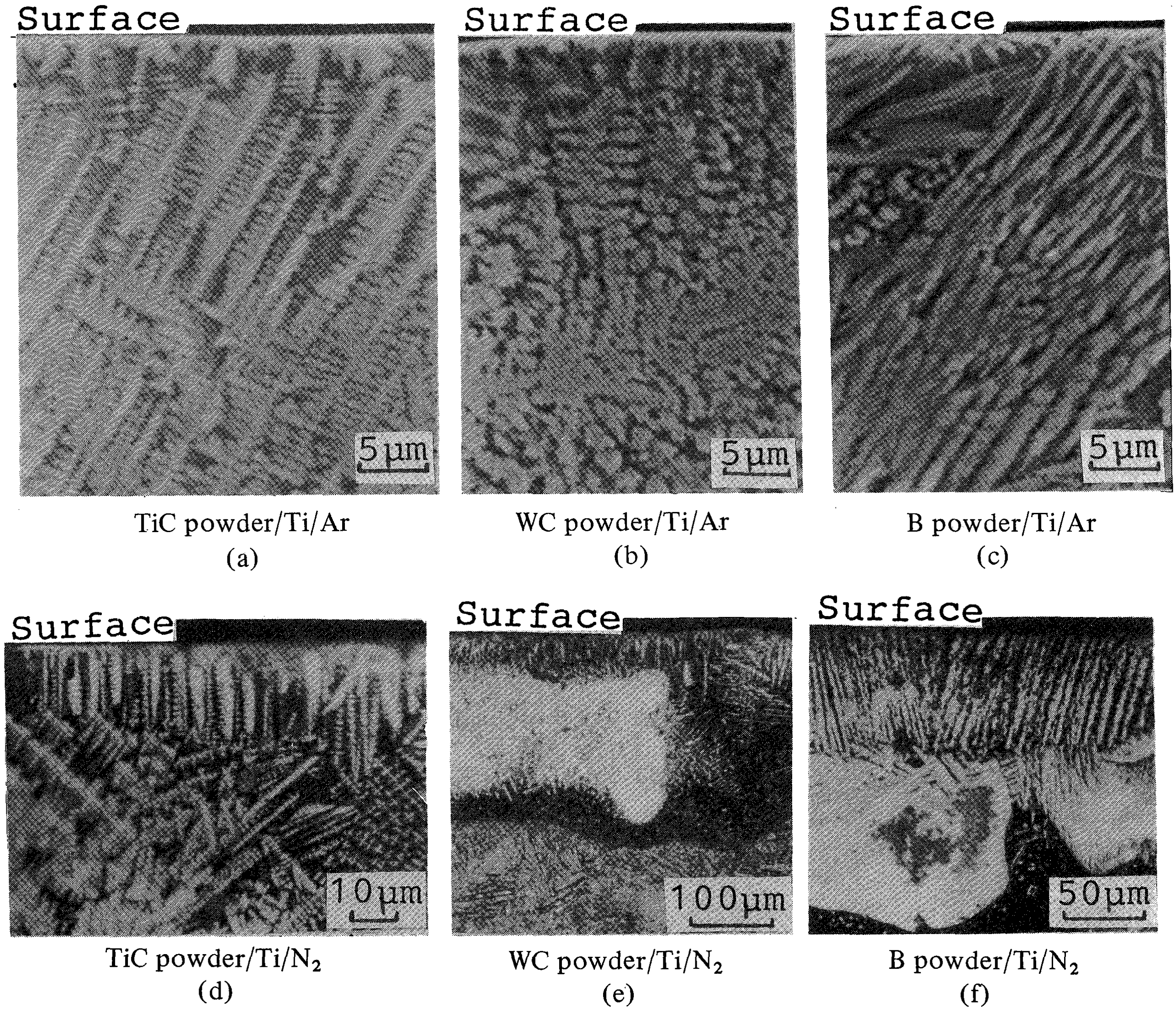

Fig. 4 Fusion zone cross-section of TiC (a, d), WC (b, e) and B (c, f) powder-predeposited Ti, irradiated by YAG laser in Ar atmosphere (a–c) and in N_2 atmosphere (e–f).

for carbides and borides, respectively. Rod shape dendrites were in the range of approximately 1 to 2μm in thickness. As shown in Fig. 4 (d) to (f), the surface appearance was modified by laser irradiation in N_2 flow; dendrites appeared to grow perpendicularly to the surface, and the thickness of such a layer was about 20 to 50μm.

Some coatings produced from borides (WB, TiB_2, B and B + C) powders occasionally contained large inclusions, which were mainly observed in the middle and at the bottom of the melted zone, as shown in **Fig. 5** (a) and (b) for B and TiB_2 powders. In the case of SiC powders, no inclusions were found at all. These inclusions seem to be brittle and may present some cracks. **Figure 6** is a photo of cross section after laser treatment of WB

Table 2 Description of dendrites shape in the laser fusion zone for different powder compositions.

Powder	Laser fusion zone microstructure	Powder	Laser fusion zone microstructure
C	Granular microstructure	B	Rod shape
TiC	Skeleton shape	TiB_2	Rod shape
WC	Flake and skeleton shape	WB	Rod and flake shape
SiC	Flake and skeleton shape	B + C	Rod and feather shape

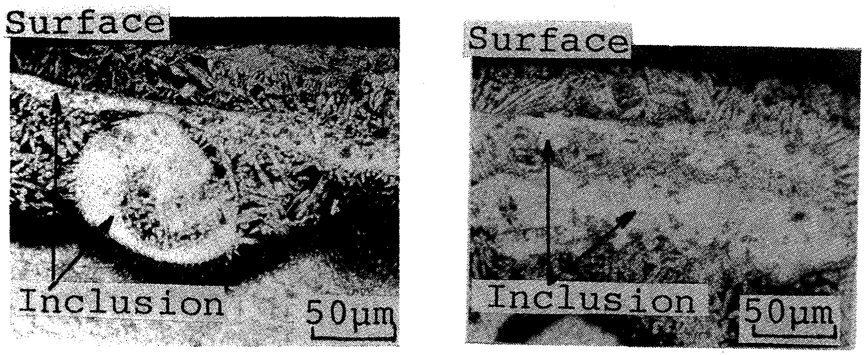

B powder/Ti/Ar
(a)

TiB_2 powder/Ti/Ar
(b)

Fig. 5 Fusion zone cross-section of B (a) and TiB_2 (b) powder-predeposited Ti, irradiated in Ar atmosphere showing large inclusions.

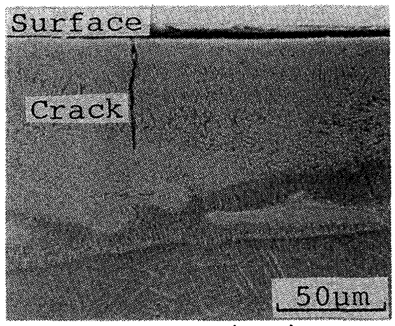

WB powder/Ti/Ar

Fig. 6 Crack in the fusion zone of WB powder-predeposited Ti, irradiated by YAG laser in Ar atmosphere.

powder-predeposited Ti in Ar flow, showing a typical crack in fusion zone. Cracks were observed on coatings surface, except for C and WC predeposited Ti.

3.3 Identification of constituents in laser fusion zone

Figures 7 and 8 show SEM microstructures and EDX results of laser-treated zones of WC and WB powder-predeposited Ti in Ar flow. W and Ti elements were detected in the fusion zone, which confirms that coating was produced by melting powders and Ti substrate. In the case of WC and WB predeposited Ti, inclusions were enriched in W but depleted in Ti in comparison with dendritic zones. Especially in the surface surroundings of WB powder-predeposited Ti, the W concentration was highly increased and Ti content was accordingly decreased. Other EDX results showed that dendrites and inclusions have almost the same composition in the case of elements (B, C, B + C) and Ti-based powders.

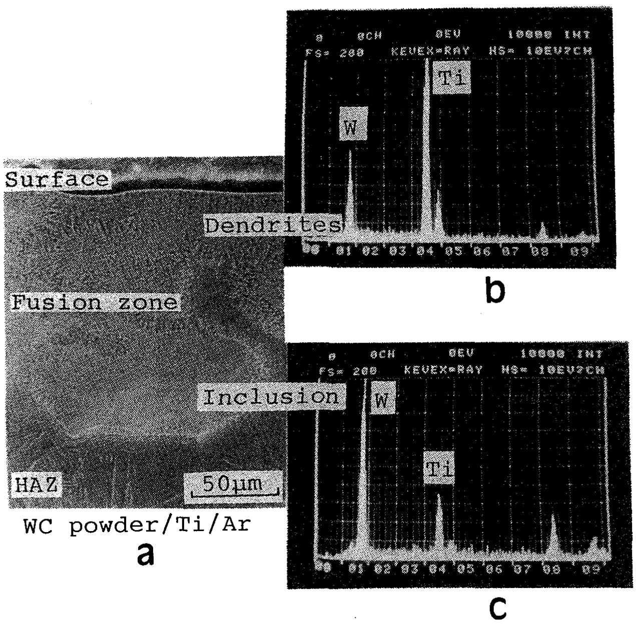

Fig. 7 Fusion zone cross section (a) of WC powder-predeposited Ti, irradiated in Ar atmosphere, and corresponding EDX analysis in the vicinity of the surface (b) and the bottom (c).

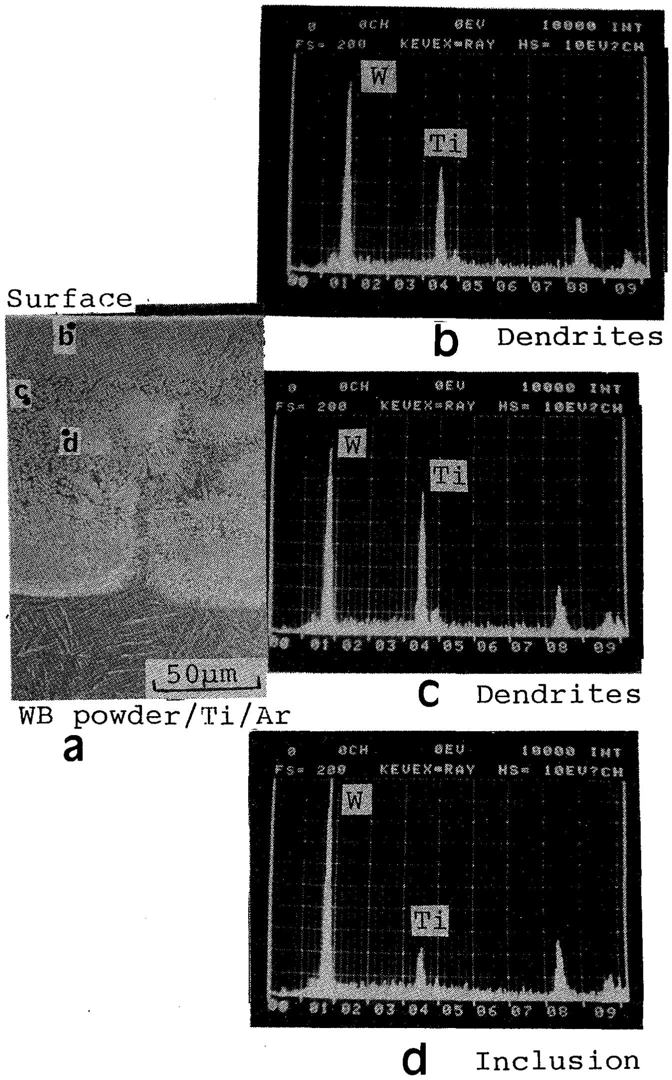

Fig. 8 Fusion zone cross-section (a) of WB-predeposited Ti, irradiated in Ar atmosphere, and corresponding EDX analysis near the surface (b), in a dendritic zone at about 50μm from the surface (c) and in an inclusion in the middle part of the fusion zone (d).

Subsequently, phases near the surface of laser-treated specimens were identified by X-ray diffractometer. **Figure 9** indicated the analytical results for B powder, showing the formation of TiB and TiB_2 in Ar atmosphere (a) and furthermore TiN in N_2 flow (b). These X-ray diffraction results in Ar were summarized in **Table 3**. In the case of WC, SiC and WB, for example, TiC and TiB were detected in addition to compounds containing the same composition as initial powders. This observation suggests that powder may be decomposed in its elements which then react with the titanium substrate.

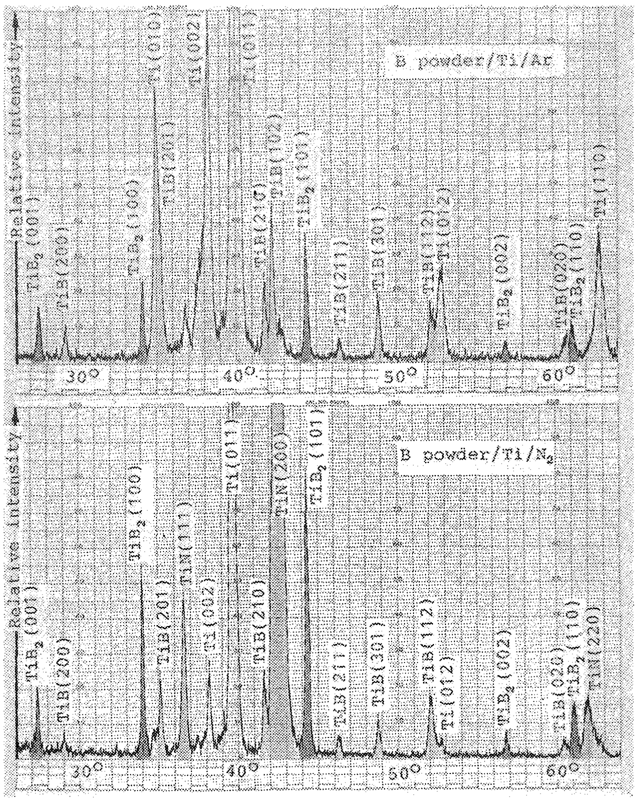

Fig. 9 X-ray diffraction analysis of B powder-predeposited Ti, irradiated in Ar (a) and in N_2 (b) atmosphere.

Table 3 X-ray diffraction analysis of ceramic coatings, after irradiation of powder-predeposited titanium substrate, by pulsed YAG laser, under argon atmosphere.

Powder	Constituents	Powder	Constituents
C	α-Ti, (TiC)	B	TiB_2, TiB, α-Ti
TiC	TiC, α-Ti	TiB_2	TiB_2, TiB, α-Ti
WC	β-WC, W_2C, TiC, α-Ti	WB	δ-WB, W, (α-Ti, TiB)
SiC	SiC, TiC, Ti_5Si_3, ($TiSi_2$)	B + C	TiB_2, TiB, (TiC, α-Ti)

3.4 Hardness of laser fusion zone

The fusion zone profile hardness shows that the microhardness values generally decrease from the surface to the bottom of the melted zone, as indicated in **Fig. 10**. In the case of laser irradiation in Ar atmosphere, this hardness decrease may be correlated to a decrease in dendrites density from the surface to the bottom. Mean hardness values measured on the surface and dendritic zone in the middle part of the fusion zone are summarized for different powder compositions in **Fig. 11**. Most surface hardnesses reached values higher than Hv = 700 (Ti hardness: Hv = 200). However, in the case of C, TiC and WC of small powder size, the surface hardnesses were about Hv = 350–500. **Figure 12** shows a comparison between dendritic zone and inclusion hardnesses obtained with B powder in Ar flow. By comparison, hardnesses measured in inclusions reached values higher than Hv > 2000.

When samples were irradiated in N_2 atmosphere, an increase in surface hardness was observed, as indicated in **Fig. 13** and **Fig. 14** in comparison with Fig. 10 and 12.

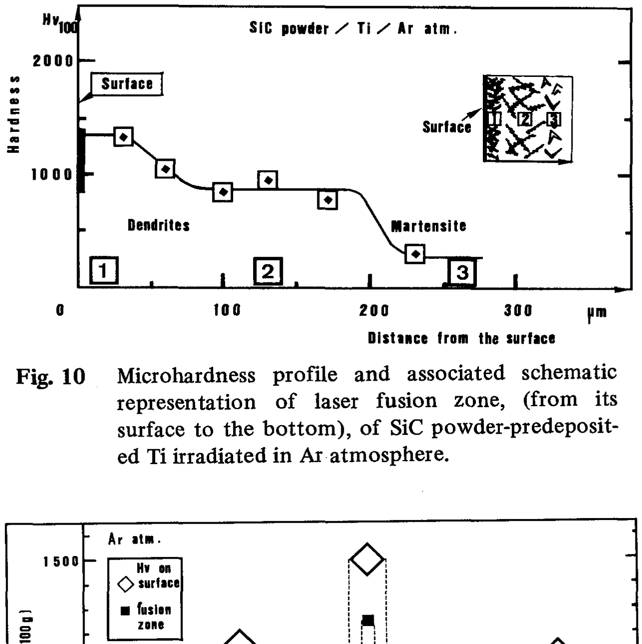

Fig. 10 Microhardness profile and associated schematic representation of laser fusion zone, (from its surface to the bottom), of SiC powder-predeposited Ti irradiated in Ar atmosphere.

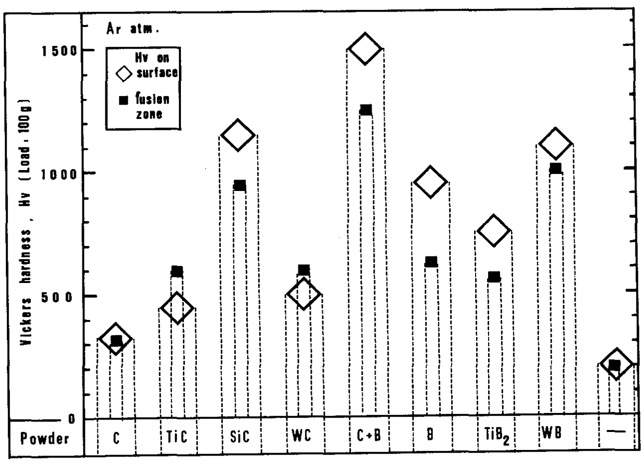

Fig. 11 Microhardness of dendritic zone on the surface and the middle of the fusion zone, depending on the initial powder composition.

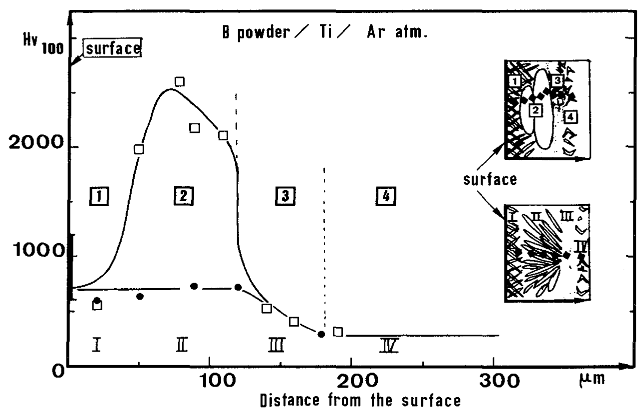

Fig. 12 Microhardness profile and associated schematic representation of laser fusion zone of B powder-predeposited Ti, irradiated in Ar atmosphere, showing the existence of hard inclusions at the bottom of the fusion zones.

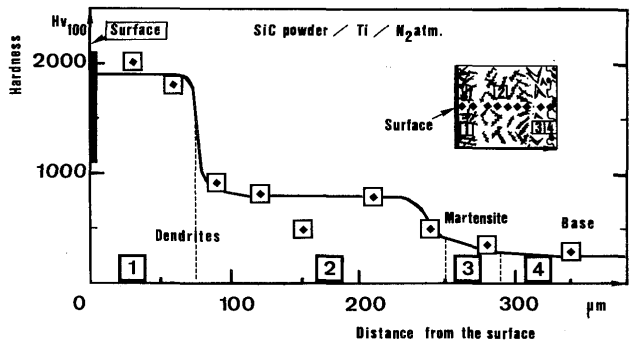

Fig. 13 Microhardness profile and associated schematic representation of laser fusion zone, (from its surface to the bottom), of SiC powder-predeposited Ti irradiated in N_2 atmosphere.

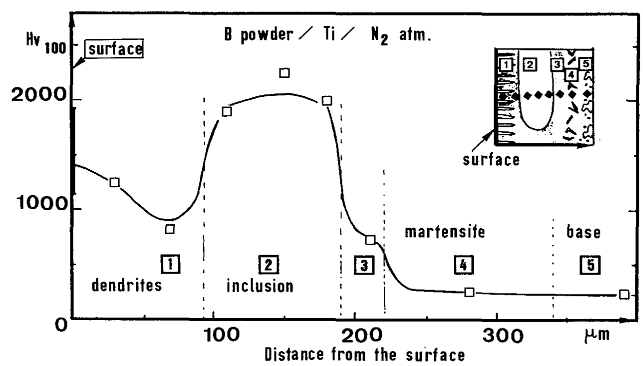

Fig. 14 Microhardness profile and associated schematic representation of laser fusion zone of B powder-predeposited Ti, irradiated in N_2 atmosphere, showing the existence of hard inclusions at the bottom of the fusion zones.

However, hardness (and microstructure) of the bottom of the melted zone did not seem to be influenced by using N_2 atmosphere. **Figure 15** shows a comparison of average surface hardnesses between Ar and N_2 atmosphere. In N_2 flow, the increase of about Hv = 500 in surface hardness was obtained for the different powder compositions, except in the case of WB powder. This reason is attributed to the formation of a surface layer rich in TiN (as described in Section 3.3). In case of WB-predeposited Ti, the fact, that no increase in surface hardness was observed in N_2 atmosphere, may be attributed to the excess of W in the surface, i.e. the low Ti concentration which might be able to react and give TiN, as already shown by X-ray analysis and confirmed by EDX analysis in Fig. 8 (compare with WC case in Fig. 7).

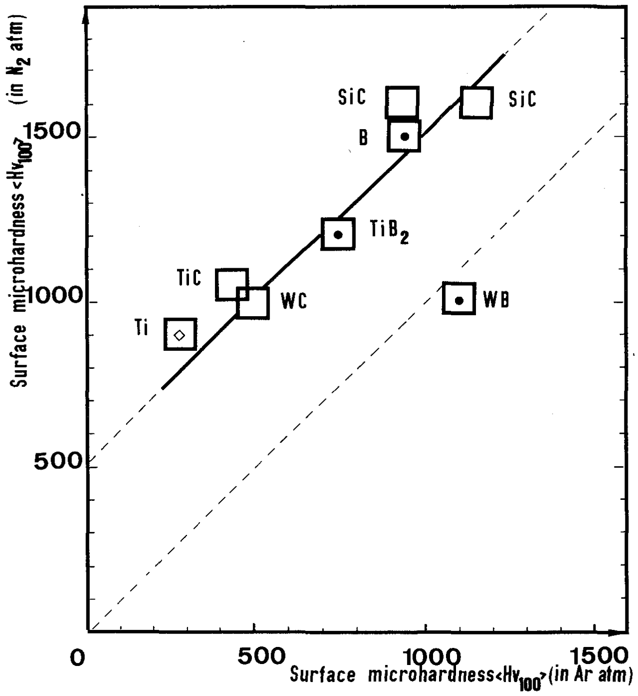

Fig. 15 Influence of using N_2 instead of Ar atmosphere during laser irradiation on the surface microhardness.

4. Conclusion

In order to improve the erosion and wear resistance of titanium, ceramics coatings were performed by pulsed YAG laser irradiation onto carbides or borides powders predeposited titanium under argon (Ar) or nitrogen (N_2) atmosphere. Coatings microstructure was mainly dendritic with some inclusions. Depending on the powder compositions, the surface microhardnesses were increased from 500 to 1200 kg/mm^2 in Ar atmosphere because of the formation of ceramic dendrites. Furthermore the hardnesses were enhanced from 1000 to 1700 kg/mm^2 in N_2 atmosphere due to the additional formation of TiN; nevertheless, inclusions hardness reached value higher than 2000 kg/mm^2.

References

1) D. Eylon, S. Fujishiro, P. J. Postans and F. H. Froes: "High Temperature Titanium alloys: A Review", Journal of Metals, Nov. (1984), 55–62.

2) J. R. Myers, H. B. Bomberger and F. H. Froes: "Corrosion Behavior and Use of Titanium and its Alloys", Journal of Metals, Oct. (1984), 51–60.

3) D. W. Richardson: "Evolution in the U. S. of Ceramic Technology for Turbine Engines", Ceramic Bulletin, Vol. 64 (1985), 282–286.

4) D. R. Johnson and R. B. Schulz: "Structural Ceramic Research and Development in Japan", Ceramic Bulletin, Vol. 64 (1985), 376–379.

5) C. W. Draper and J. M. Poate: "Laser Surface Alloying", International Metal Reviews, Vol. 30 (1985), 85–108.

6) K. P. Cooper and J. D. Ayers: "Laser Melt-Particle Injection Processing", Surface Engineering, Vol. 1 (1985), No. 4, 263–272.

7) A. Walker, J. Folkes, W. M. Steen and D. F. West: "The Laser Surface Alloying of Titanium Substrates with Carbon and Nitrogen", Surface Engineering, Vol. 1 (1985), No. 1, 23–29.

8) S. Katayama, A. Matsunawa, A. Moritomo, S. Ishimoto and Y. Arata: "Surface Hardening of Titanium by Laser Nitriding", Proc. ICALEO, ILA, Vol. 38 (1983), 127–134.

9) A. Dearnley and T. Bell: "Engineering the Surface with Boron based Materials", Surface Engineering, Vol. 1 (1985), No. 3, 203–217.

10) J. Com-Nougué, E. Kerrand, F. Gariou and M. Guilloussou: "CO_2 Laser Deposition of a Cobalt Base Alloy on a 12% Chromium Steel", 3nd International Conference on Lasers in Manufacturing, 3–5 June, Paris, France.